

## Failure Detection in Energized High Voltage Substation Grounding Grids - A Case Study

Luana Vasconcelos Gomes<sup>1</sup>, Euler C. T. Macedo<sup>2</sup>, Edson Guedes da Costa<sup>1</sup>,  
Raimundo Carlos Silvério Freire<sup>1</sup> and Malone Soares de Castro<sup>1</sup>  
<sup>1</sup>(Postgraduate of Electrical Engineering/Federal University of Campina Grande, Brazil)  
<sup>2</sup>(Department of Electrical Engineering/Federal University of Paraiba, Brazil)

---

**Abstract:** An electronic system of measuring and processing surface voltage potentials distributed along the grounding grid was developed. The electronic system is composed of several parts, an embedded computer, signal conditioning circuits and computational routines. The adopted processor was a low-power open-source single-board computer that allows the implementation of routines based on the finite-difference method. It was possible to create two real time dimensional plots using the fall-of-potential method. The electronic system was able to make a correct diagnosis of the aging state of the grounding grid. The results allowed evaluation of the potential behaviour of the ground surface voltage in a consistent manner in a steady state operation. The results obtained from measurements in high voltage substations using the developed embedded system were satisfactory when compared to other measuring devices. This system was capable of easily locating problematic zones, such as high potential concentrations, allowing efficient and fast grounding grid diagnosis.

**Keywords:** diagnostic, grounding grid degradation, high voltage grounding, substation, surface voltages

---

### I. Introduction

The introduction most equipment found in a high voltage substation uses the ground connection as a reference for all operational voltages in the system. From an operational safety point of view, the objective of a ground grid is to allow safe equipotential surface voltage on the ground during a surge (e.g. atmospheric and switching surges) and when an industrial frequency current is flowing to the grounding.

A poor grounding system not only results in unnecessary transient damage, but also causes data and equipment loss, plant shutdown, and increases fire and personnel risk[1]. An efficient grounding system can impact on better energy quality rate. A low ground resistance value is not a guarantee of safety, because there is no direct relationship between the grounding resistance and the maximum electric current that a person is capable of surviving[2]; based on this, alongside the necessity of verifying ground resistance during inspections, it is necessary to evaluate the grid conductor condition and its connection points. The difference of potential between different substation positions must mitigate personal safety and the adequate operation of equipment installed in high voltage substations.

Based on their importance in relation to the system's operational continuity, grounding grids require periodic evaluation, not only based on conductor corrosion, but also on ground resistivity and soil imperfections (e.g. rocks, soil composition, soil inclination, etc.).

Some analytical methods are now being implemented in computational routines. Most of these methods try to simulate real situations in grounding systems, promoting an additional analysis to the practical measurement method[3-8]. Many papers deal with the monitoring and diagnosis of the operational conditions of grounding grids[1], [9-16].

An indirect manner of evaluating the degradation level of a grounding grid is to analyze the potential surface distribution in the substation area and its surroundings. Grids that possess a uniform potential distribution and low ground resistance do not present degradation problems, however, an elevated potential concentration might indicate degradation [9], or other problems, such as rocks, unsuitable soil composition, etc.

A methodology that allows the detection of failures in energized grounding grids in real time is presented. Therefore, an electronic device was specially developed for this application, which measures and processes the surface potentials of an energized high voltage substation. The device is capable of measuring several points of surface potential distributed along the grounding grid, performing the surface potential mapping in order to identify high resistivity and degradation zones, discontinuities in the grid or failure points. The measured data is processed with the aid of embedded software based on the Finite Difference Method. The measurements are performed at industrial frequency and use the substation transformer unbalance current as a reference for ground potential elevation.

## II. Grounding System Theory

### 2.1 Grounding Grids

Grounding systems must be projected to allow the surface potential in a high voltage substation to stay under the maximum potential limits allowed for safety. The surface potential values must be limited in steady state and transient conditions. To satisfy the low ground resistance values and to obtain low touch and step potential values, high voltage substations are normally projected with ground grids composed of horizontal cables that connect all copper electrodes. The grounding grids are efficient and economic, and are adopted in all kinds of substations.

The IEEE standard [17] defines some important concepts in relation to the electric potential distribution:

- Step voltage: The difference in surface potential experienced by a person bridging a distance of 1 m with their feet without contacting any other grounded object.
- Touch voltage: The difference of potential between the ground potential rise (GPR) and the surface potential at the point where a person is standing, while at the same time having their hands in contact with a grounded structure.
- Mesh voltage: The maximum touch voltage to be found within a mesh of a ground grid.
- Transferred voltage: A special case of touch voltage where voltage is transferred into or out of the substation.

In a grounding grid, the current flows preferentially through the edges. The typical equipotential distribution lines inside and in the neighboring region of the ground grid are given in **Error! Reference source not found.1**.

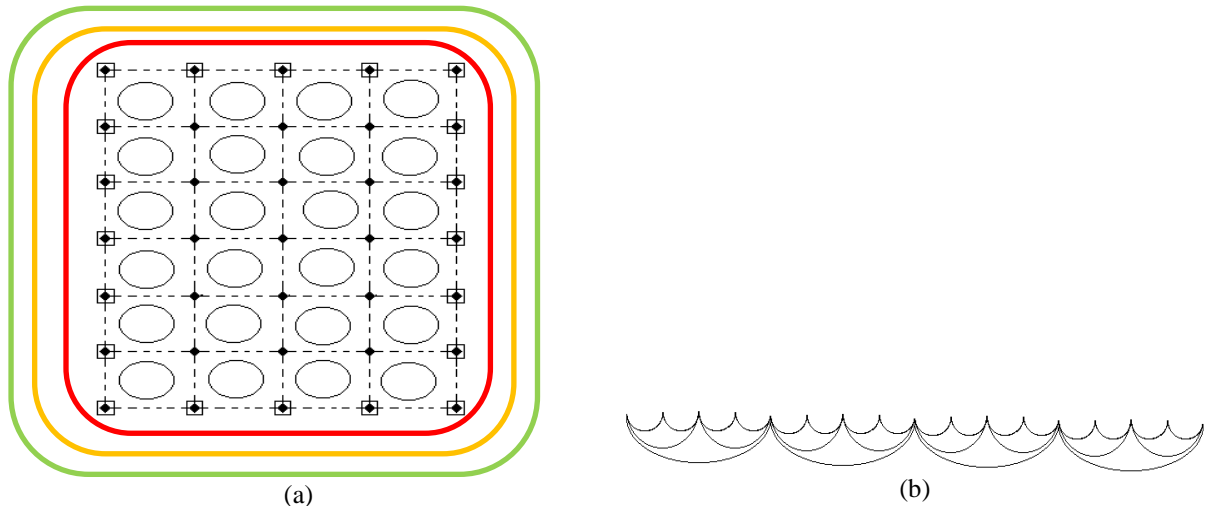


**Figure 1.** Equipotential distributions lines: (a) Equipotential lines (b) Potentials inside and in the neighboring regions of a ground grid.

### 2.2 Finite Difference Methods (FDM)

To determine the electric potential in a region when the potential  $V$  is known only in certain points of the region under analysis, either a Poisson Equation (1) or a Laplace equation (2) is used [18], [19]. [9] presents the mathematical development and the computer simulation steps.

The surface potential mapping of a region of interest is obtained by performing the Laplace equation solution using the Finite Difference Method. The solution is performed in four steps. The first step consists of dividing the interest region into node grids, as seen in **Error! Reference source not found. 2**.

In the second step, the contour conditions are established, attributing nodes, called ‘fixed nodes’ to the grid extremity of the region. Internal nodes are termed ‘free nodes’.

In the third step, it is necessary to obtain approximations by calculating the finite difference of the Poisson differential equation. In case  $\rho_s = 0$ , the finite difference approximation of the Laplace Equation is obtained, as illustrated by (1):

$$V_{i,j} = \frac{1}{4}(V_{i+1,j} + V_{i-1,j} + V_{i,j+1} + V_{i,j-1}) \quad (1)$$

The Laplace finite difference equation is determined for each point of the discretized region for which it is desired to calculate the problem solution.

The fourth step consists of iteratively calculating the potential values at all grid nodes.

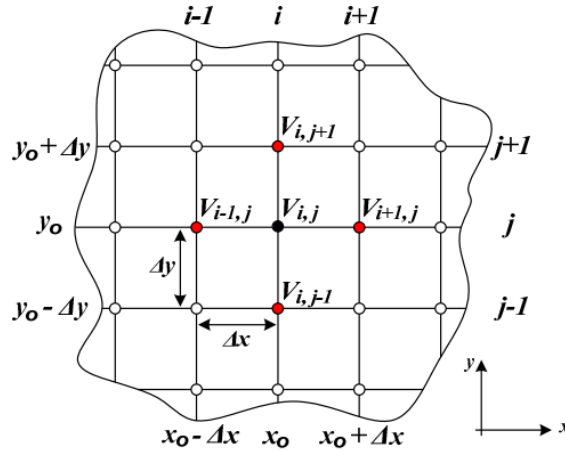


Figure 2. Domain discretization [18].

### III. Material And Methods

[9] presents the embedded system development with the several technologies employed. A block diagram of the developed system is presented in Fig.3. In the sequence, each block of the measurement system is detailed.

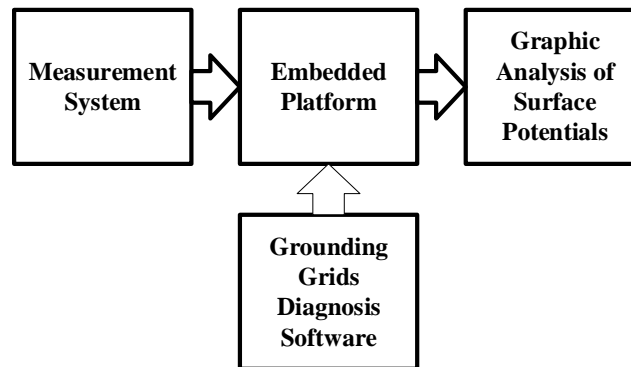


Figure 3. Embedded electronic system block diagram.

#### 3.1 Measurement System

The measurement system procedure is composed of signal conditioning circuit plus protection; analog multiplex; PIC microcontroller; serial/USB communication and a Beagle Board.

The conditioning circuit is composed of resistors and operational amplifiers and allows the attenuation of input signals. The measurement system operates with eight different scales, and the correct scale selection is performed automatically by the microcontroller. Initially, the scale is tested in its lower value and then is automatically changed until the detection of the appropriated scale value. The PIC 18F452 microcontroller is responsible for automatically controlling the scales using an analog multiplexer, performing the peak detection, coordinating and executing the measurement process and transferring the measured data to the embedded system (the Beagle Board, using the RS232/USB communication protocol). The functional block diagram of the measurement system is presented in **Error! Reference source not found.** 4.

To perform the surface potential measurement efficiently, specific procedures were adopted in the process:

- Automatically repeating the measurement and calculating the arithmetic mean of the obtained data, to avoid incorrect values. If the calculated mean result is not consistent, the data is discarded and the procedure is repeated.
- Verifying whether the mean of the measured values is in the range of  $\pm 10\%$  of the fifth digit of the measurement value, to filter harmonic components from the measurement data.

#### 3.2 Embedded Platform

The Beagle Board is equipped with the basic functionalities of a computer [20]. It is employed in several embedded system technologies. The descriptions of the technical characteristics of the Beagle Board used as a

coordinator system are found in [9], but, with the objective of maintaining the low-cost development, an open-source Linux® operational system was used, the Angstrom® distribution.

### 3.3 Grounding Grid Diagnosis Software

The software must be able to map the potential at the ground surface of the substation and its neighborhoods. The diagnosis enables possible field concentrations or eventual difficulties for current draining to be noted, such as high resistivity zones in the grid area, corrosion or discontinuity in steady-state operation condition or in a short-circuit occurrence.

The computational routine was developed by using a multiplatform tool, the Qt®, which is widely used for the application development of graphical user interfaces (GUI), in embedded systems. The tools adopted were the QT Creator platform, C++ language and the Qwt graphical library (Qt Widgets for Technical Applications). The Qwt library possesses several types of data structures for bi-dimensional data plotting. These features include curve plots, scatter plots, spectrograms, contour plots, histograms, dials, compasses, knobs, wheels, sliders, thermos, etc.

In order to use the software, the specification of a domain, contour conditions and/or initial conditions are necessary. Using these conditions associated with computational resources, it was possible to simulate the behavior of the electric potential (V) in a determined region, in this case, the HV substation [9] - [16].

Fig. 5 shows the second software window when the user has selected the measurement point. With a virtual keyboard, the user enters the coordinates of the measured point. The graphic is generated after the selection of the Graphic button. The flowchart of the measurement procedure is presented in Fig. 6.

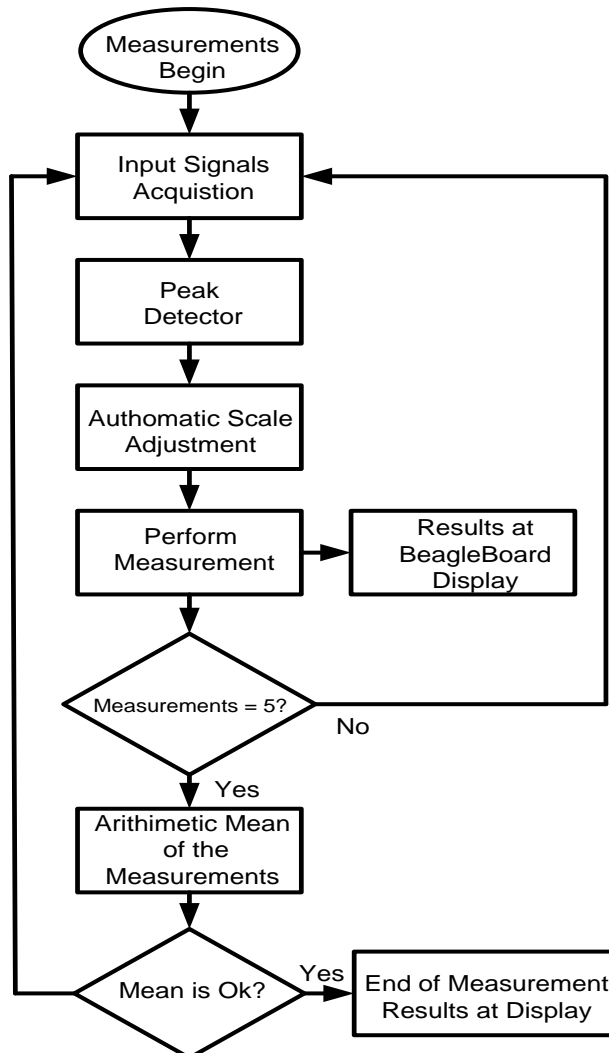


Figure 4. Block diagram of the measurement system.

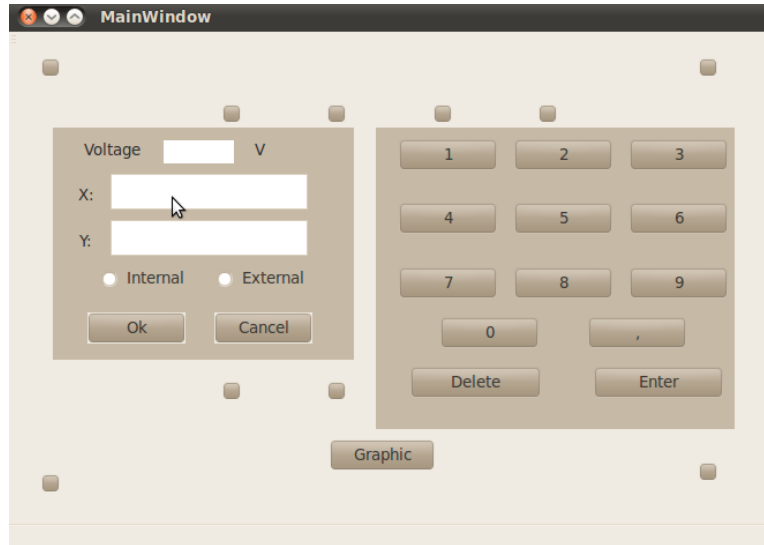


Figure 5. Measurement system user interface.

### 3.4 Graphic Analysis of Surface Potentials

The surface potential of the graphical analysis of three cases is shown in the results and discussion section. The behavior of the grounding grid in normal steady-state operational conditions, analysis of the occurrence of a fault in the grounding grid with a discontinuity, and the analyses and diagnoses of an energized 69/13.8 kV high voltage substation will be shown.

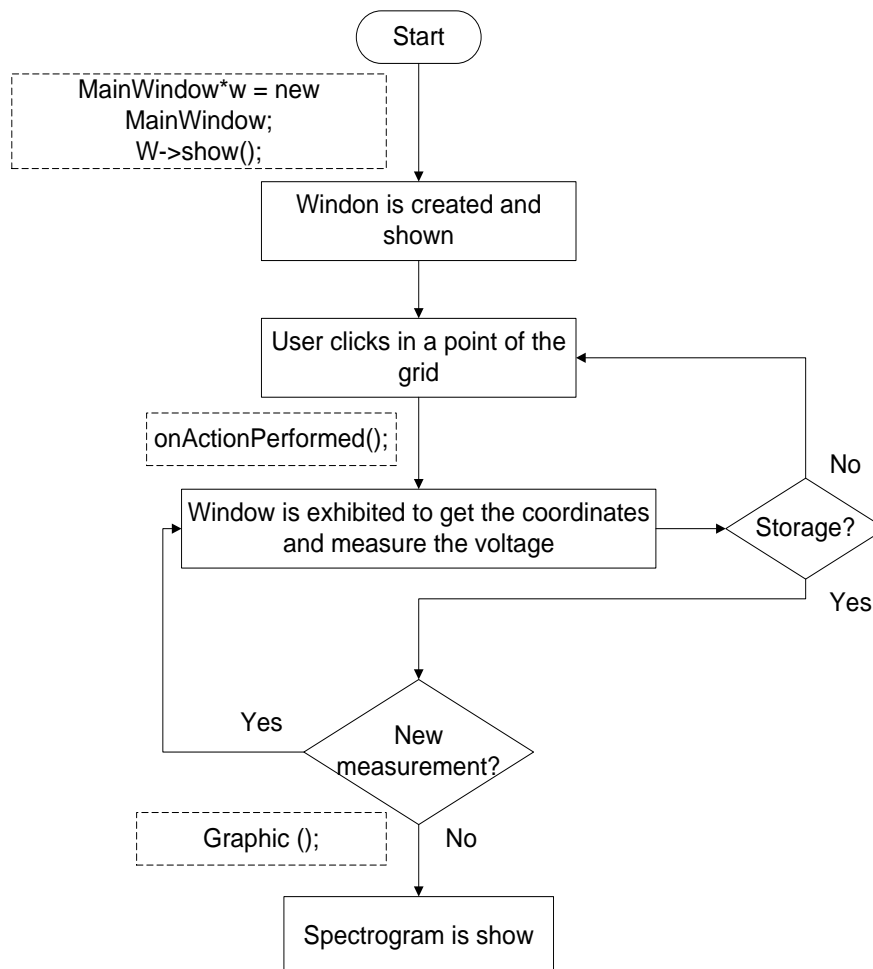


Figure 6. Measurement procedure flowchart.

#### IV. Results And Discussion

This section presents some results obtained using the developed system. The main results are the evaluation of measurement data. The grounding grid surface potential measurements were performed on the patio of the High Voltage Laboratory at the Federal University of Campina Grande, and at a 69/13.8 kV energized substation.

With the objective of evaluating the performance of the developed embedded system, several measurements were initially taken in a ground grid composed of three copper rods of 1.2 m in length, placed in an equilateral triangular configuration. The ground grid was installed in heterogeneous soil with a resistance equal to 8.46  $\Omega$ , with 2.5 m side and the electrodes were buried 50 cm deep. The tests were performed using a Variable Voltage Transformer (variac) that tries to simulate the unbalanced current injected.

The system was evaluated in three different cases:

- A grounding grid under normal steady-state operational conditions (i.e. without surges and grid defects), labelled Case 1.
- The occurrence of a fault in the ground grid with a discontinuity was simulated in Case 2.
- The third situation (Case 3) consisted of several measurements, analyses and diagnoses of an energized 69/13.8 kV high voltage substation.

##### 4.1 Measurement System Evaluation

Initially, to verify the accuracy of the measurements made by the developed system, several measurements were taken simultaneously using a Tektronix® digital oscilloscope TDS 2024B model. The comparison between the two measurement systems is presented in Table 1. Data was obtained using the setup presented in **Error! Reference source not found.7**.

**Table 1** Comparison between the performed measurements using the developed embedded system and an oscilloscope

Measurement Points	Embedded System	Oscilloscope	Error (%)
1	5.80	6.00	3.40
23	5.30	5.60	5.30
31	7.94	8.40	5.40
39	9.00	9.50	5.30
45	10.60	11.20	5.35
50	15.80	16.40	3.70
53	16.40	17.20	4.65
57	21.85	22.40	2.50
63	25,60	26.20	2.30
69	30.45	31.20	2.42

The error percentage was calculated in relation to the measured values arithmetic mean. It was confirmed that sometimes the measurement results obtained using the oscilloscope presented variations (spikes, noise, etc.). The results presented in Table I correspond to the arithmetic mean of five measurement results. The same procedure was automatically adopted by the developed system.

As the obtained results were considered satisfactory, the experimental setup presented in Case 1 was performed: the complete analysis of a grounding grid under normal operational steady-state conditions (without surges and grid defects).

Case 2 was then analyzed. The same grounding grid presented in Case 1 was considered, but a discontinuity zone was inserted.

In Case 3, several measurements were taken in an energized substation, with a special characteristic: the measurements were taken at different periods of time, during the humid and dry seasons.

In the following sections, the results obtained in the three distinct situations are detailed.

##### 4.2 Case 1 – Grounding Grid in Steady State

For adequate computational routine processing, the determination of the correct position of each measurement point (geographic coordinates of the measurement point) is necessary to create a simplified scheme (sketch), as presented in **Error! Reference source not found.7**. In this figure, for example, the number of measurement points and their coordinates (x and y), the position where the electrodes are installed, and the grid dimensions, etc., are presented.

The potential surface measurements were performed in accordance with Section III. The main goal of this procedure was to verify the functionality of the developed embedded system and to measure and map the potential distribution on the ground to indirectly assess the degradation of the grounding grid.

During the experimental setup, 91 measurements were taken, spaced 1.5 m apart. The reference point was positioned 48 m from the ground grid, and an unbalanced current of 5 A was injected into the ground.

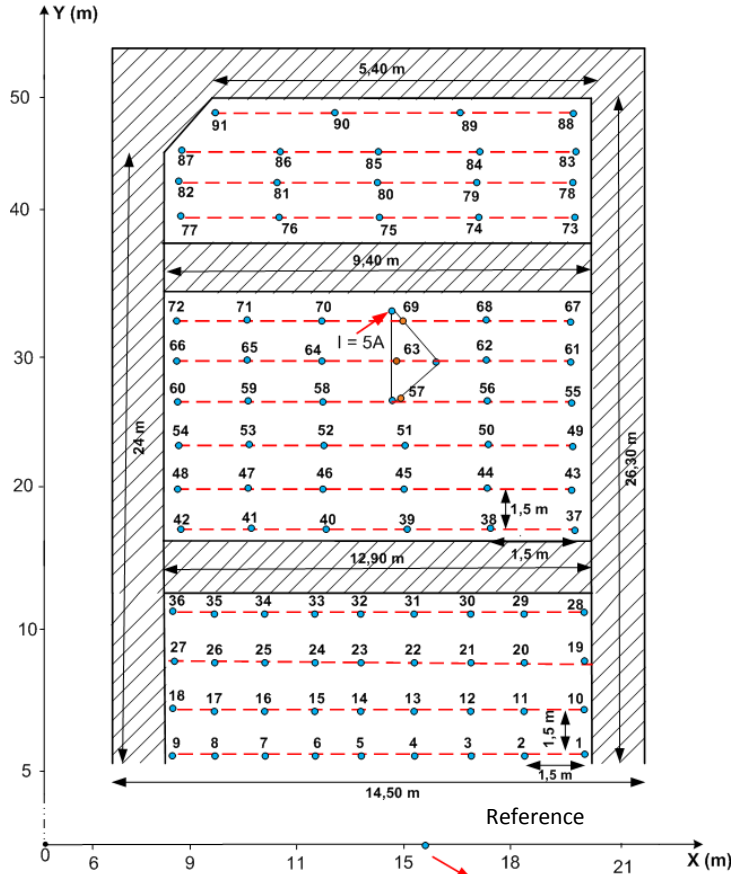


Figure 7. Surface potential measurement points from a steady-state laboratory grounding grid (no defects).

The results obtained with the proposed embedded system, for steady state operation are presented in Figs. 8 and 9. In these figures, the surface potential distribution and the equipotential lines found on the ground are presented, respectively. In Fig.10the combination of the two previous figures is presented.

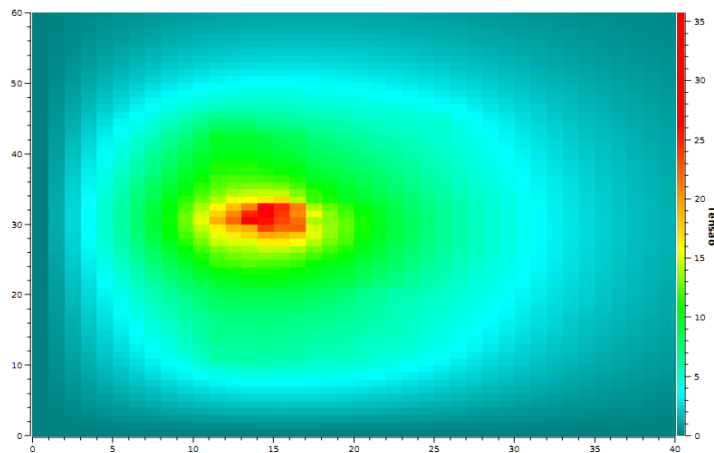


Figure 8. Surface potentials levels of a grounding grid without defects.

The results obtained demonstrate that the surface potential distribution and the equipotential lines are uniform, since elevated values of voltage were detected in the points near the grounding grid, where the 5A current was

injected, and with an increase in distance the surface potential gradually decreased. This behavior demonstrates the adequate current flow in the ground.

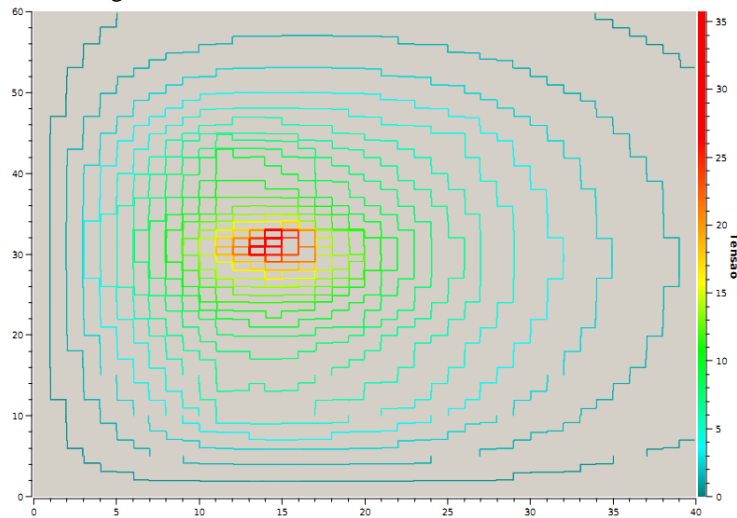


Figure 9. Equipotential lines of a grounding grid without defects.

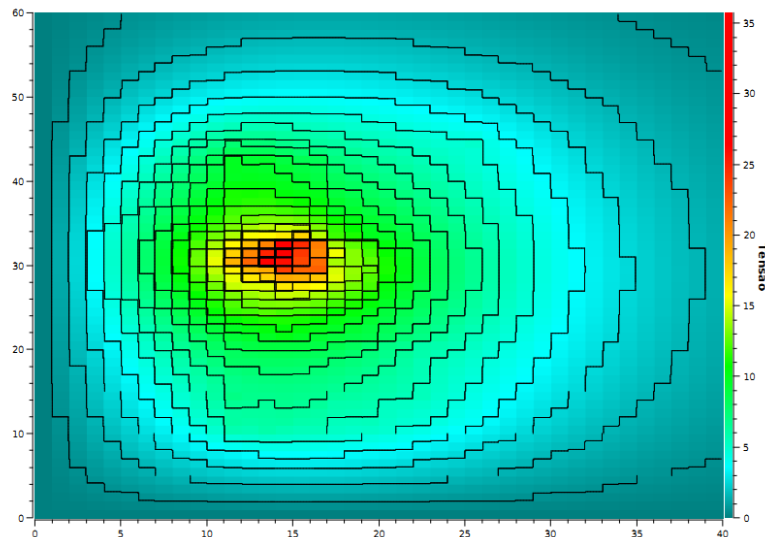


Figure 10. Result obtained combining the surface potential levels and the equipotential lines of a grounding grid without defects.

#### 4.3 Case 2 – Grounding Grid with Discontinuity

In order to evaluate the performance of the developed embedded device in grounding grid with a discontinuity zone, the same grounding grid configuration as presented in Case 1 was used. A defect zone was generated by inserting an electrode with a 12 m distance from the grounding grid, where a 1.3 A current was injected, as seen in Fig.11.

The results obtained are presented in Figs.12, 13 and 14. In these figures the surface potential distribution, the equipotential lines and the combination of the previous figures in a single graph are illustrated.

Analyzing the results from Case 2, it is possible to verify a region with elevated surface. A concentration of equipotential lines was also verified. The results confirm that the developed device allows the identification of areas with an elevation of surface potential in a grounding grid, thereby providing an efficient diagnosis.

#### 4.4 Case 3 – Results obtained from an Energized High Voltage Substation

The surface potential measurements in an energized substation were taken using the same procedure presented in Case 1 and 2, but in two distinct seasons, with an interval of about six months between the measurements.

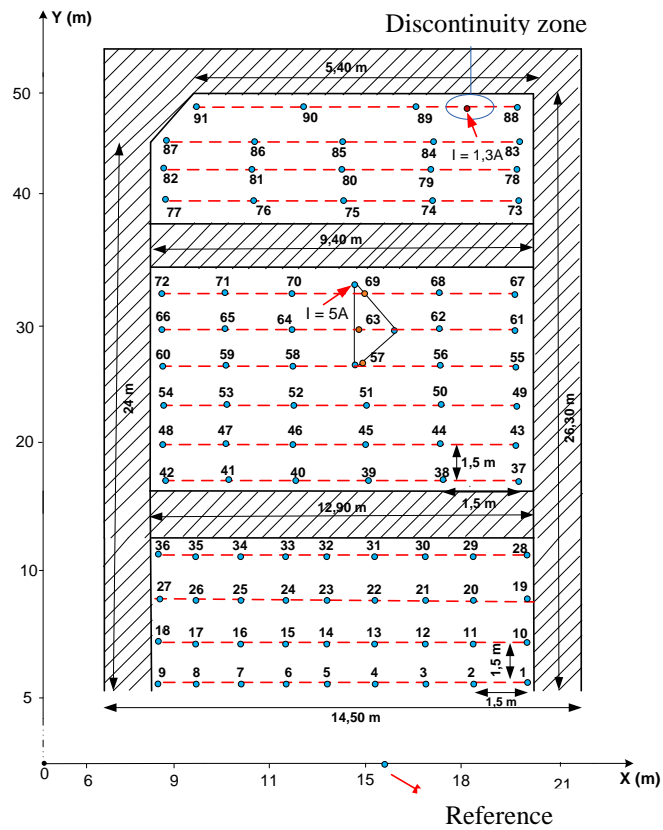


Fig.1. Surface potential measurement points from a steady-state laboratory grounding grid (with a discontinuity zone defects).

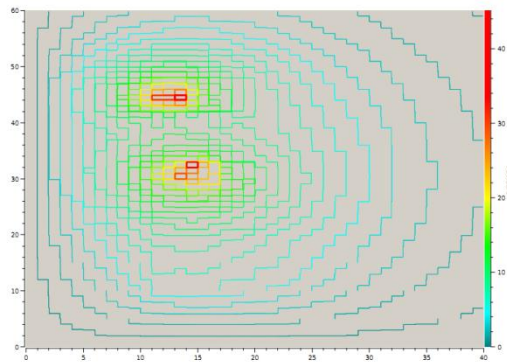


Figure 11. Surface potential measurement points from a steady-state laboratory grounding grid (with a discontinuity zone defects).

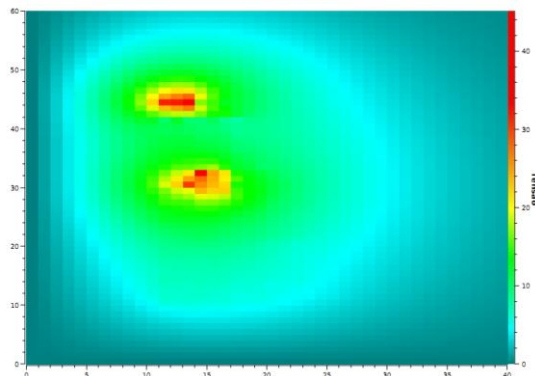
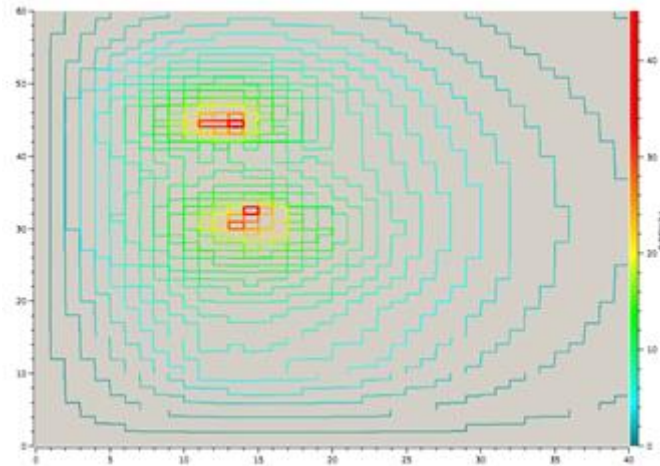


Figure 12. Surface potential levels of a grounding grid with a discontinuity zone.

The first measurement setup was carried out at the end of the rainy season and the second setup at the end of the dry period with elevated ambient temperature.

During the first setup measurements were made at 70 different points arranged in the effective area of the grounding grid and its surroundings. The test electrode was positioned in a 7x7 m mesh.

Following the same procedure used in the second setup, 118 different surface potential levels were measured in the effective area of the grounding grid and its surroundings. With the objective of obtaining a more detailed surface potential mapping, the test electrode was positioned following a 5x5 m mesh.



**Figure 13.** Equipotential lines of a grounding grid with a discontinuity zone.

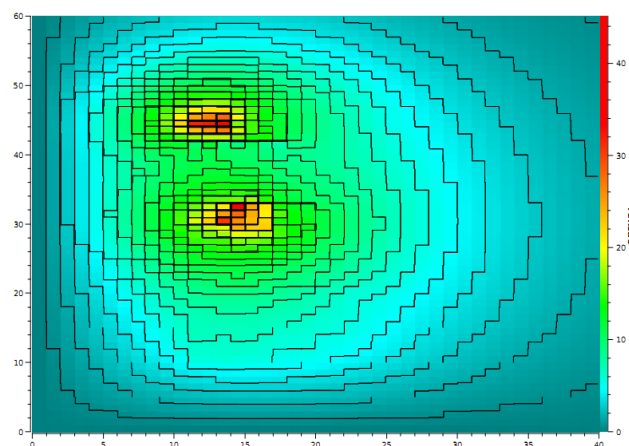


**Figure 14.** Results obtained combining the surface potential levels and the equipotential lines of a grounding grid with a discontinuity zone.

From the measured surface potential data, it was possible to map the ground surface potentials, indicating the field concentrations, both in steady state and in short circuit conditions, generating 2D graphics for both situations.

**Error! Reference source not found.** presents the 2D plots of the surface potential distribution generated by the measurements after the rainy period.

**Error! Reference source not found.** presents the 2D plots with the surface potential distribution of the energized substations in the end of the dry period.

Visual inspection showed that the surface potential mapping for the energized substation presented different results, especially for a particular region. It was verified that the results obtained during the second setup presented elevated surface potentials values in comparison to the first setup. The explanation for this is basically the geological conditions and seasonality. It is possible to confirm from the results that during the grounding grid mesh implantation, soil with lower resistivity was used, and a rock is probably located close to the surface. Water evaporation is more intense in this region, and as a consequence, soil resistivity is greater, not allowing the current to flow through the soil, and generating elevated surface potentials during the dry season.

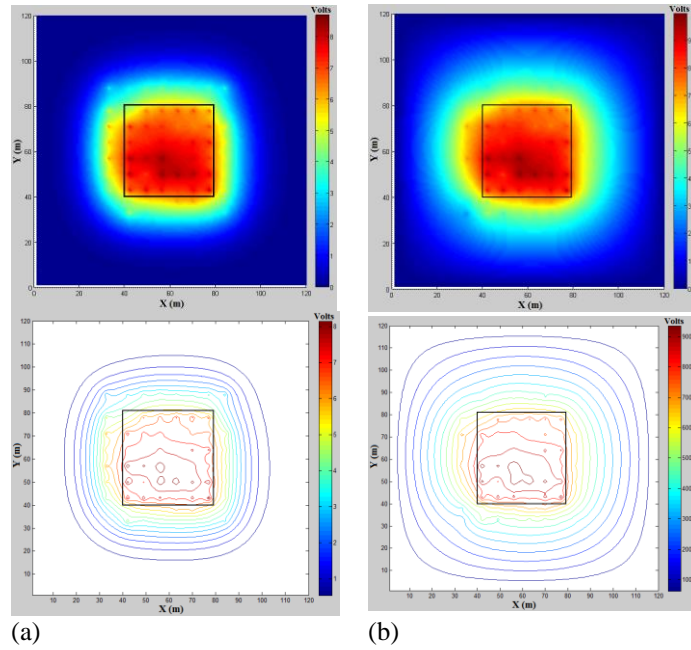


**Figure 15.** Surface potential levels and equipotential lines of an energized high voltage substation grounding after the rainy period: (a) steady state, (b) short circuit.

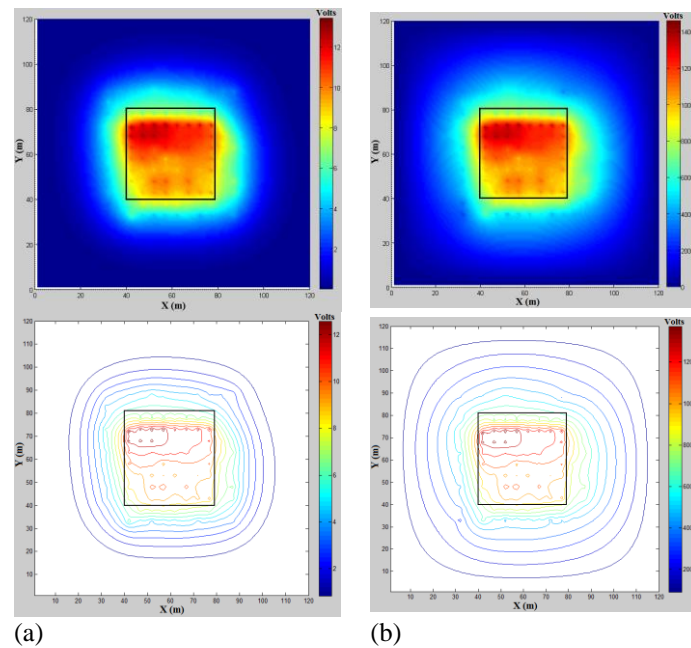


**Figure 16.** Surface potential levels and equipotential lines of an energized high voltage substation grounding after the dry period: (a) steady state, (b) short circuit.

## V. Conclusion

Substation grounding systems require permanent monitoring due to corrosion, degradation caused by high intensity current surges, seasonality, and mesh implantation conditions, such as chemical additives to reduce the original resistivity, etc.

Predictive tests on substations are increasingly difficult to perform because it is not generally possible to shut the substation down, and thus have monitoring systems that permit the real time evaluation of the operational conditions of energized substations is relevant. On the other hand, the grounding grid evaluation and determination of operational conditions is not a trivial task, because the conventional techniques of ground resistance measurement do not highlight the real conditions of the grounding grid.

A low cost system (hardware and software) was presented, and its ability to localize high resistivity zones, grid corrosion, and discontinuity zones in the grounding grid was verified. This system allows the measurement of

surface potentials and data to be analyzed using embedded software, presenting the results in 2D plots. The developed system was effective because it allowed the rapid determination of problematic zones with potential concentration, allowing a precise diagnosis of an energized 69/13.8 kV substation.

With the objective of obtaining a more accurate diagnosis and reliable operating conditions for an energized substation, several measurements were performed under different weather and humidity conditions, after dry and rainy seasons. The system highlighted the seasonality effects and geological conditions where the grid was installed, and the need for substation grounding system monitoring was demonstrated.

### References

- [1]. X. Long, M. Dong, W. Xu, Y. W. Li, "Online monitoring of substation grounding grid conditions using touch and step voltage sensors," *IEEE Trans. on Smart Grid*, vol. 3, no. 2, pp. 761–769, Jun. 2012.
- [2]. F. A.H León, M. A. P. P. Prieto and J. M. P. Quevedo, "Design and construction of a dynamic system for step and touch voltage measurements for grounding systems," in *Proc. XI SIPDA*, Fortaleza, Brazil, October 3-7, 2011.
- [3]. J. Guo, J. Zuo, B. Zhang and Z. C. Guan, "An interpolation model to accelerate the frequency-domain response calculation of grounding systems using the method of moments," *IEEE Trans. on Power Del.*, Vol. 21, no. 1, 2006.
- [4]. J. Ma and F. Dawalibi, "Analysis of grounding systems in soils with finite volumes of different resistivities," *IEEE Trans. Power Del.*, vol. 17, no. 2, pp. 596–602, Apr. 2002.
- [5]. F. Greev, R. Dawalibi, "An electromagnetic model for transients in grounding systems", *IEEE Trans. on Power Del.*, vol. 5, no. 4, pp. 1773-1781, Nov. 1990.
- [6]. C. Chang and C. Lee, "Computation of ground resistances and assessment of ground grid safety at 161/23.9-kV indoor-type substation" *IEEE Trans. Power Del.*, vol. 21, no. 3, pp. 1250–1260, Jul. 2006.
- [7]. Puttarach, N. Chakpitak, T. Kasirawat, and C. Pongsriwat, "Substation grounding grid analysis with the variation of soil layer depthmethod," in *Proc. IEEE Power Tech. Conf.*, pp. 1881–1886, Jul. 2007.
- [8]. L. Qi, X. Cui, Z. Zhao, and H. Li, "Grounding performance analysis of the substation grounding grids by finite element method in frequency domain," *IEEE Trans. Mag.*, vol. 43, no. 4, pp. 1181–1184, Apr. 2007.
- [9]. L. V. Gomes, E. C.T. de Macedo, T. C. Albuquerque, E. C. Guedes, G. V. A. Junior, M. S. de Castro and R. C. S. Freire, "Embedded system to grounding grid diagnosis of energized substations", In: *2012 IEEE International Instrumentation and Measurement Technology Conference (I2MTC)*. Austria, 2012.
- [10]. P. S. Meliopoulos, S. Patel, and G. J. Cokkinides, "A new method and instrument for touch and step voltage measurements," *IEEE Trans. Power Del.*, vol. 9, no. 4, pp. 1850–1860, Oct. 1994.
- [11]. R. Gustafson, R. Pursley, and V. Albertson, "Seasonal grounding resistance variations on distribution systems," *IEEE Trans. Power Del.*, vol. 5, no. 2, pp. 1013–1018, Apr. 1990.
- [12]. J. He, R. Zeng, Y. Gao, Y. Tu, W. Sun, J. Zou, and Z. Guan, "Seasonal influences on safety of substation grounding system," *IEEE Trans. Power Del.*, vol. 18, no. 3, pp. 788–795, Jul. 2003.
- [13]. A. D. Dias, G. V. Andrade Jr., E. G. Costa, F. P. F. Sousa, E. C. T. Macedo, L. V. Gomes, F. C. L. Brasil, "Grounding grids analysis of energized substations". in *Proc. 17th International Symposium on High Voltage Engineering - ISH 2011*. Germany, 2011.
- [14]. S. Visacro, R. Alipio, C. Pereira, M. Guimaraes, M. A. O. Schroeder, "Lightning response of grounding grids: simulated and experimental Results," *IEEE Trans. Eletromag. Comp.*, vol. 57, no. 1, pp. 121–127, Feb. 2015.
- [15]. B. D. Rodrigues, S. Visacro, "Portable grounding impedance meter based on DSP," *IEEE Trans. Instrum. and Measum.*, vol. 63, no. 8, pp. 1916–1925, Aug. 2014.
- [16]. E. C. T. Macedo, L. V. Gomes, G. V. Andrade Jr, A. D. Dias, E. G. Costa, R. C. S. Freire, M. S. Castro, "Measurement system applied to energized substations grounding grids diagnosis", in *Proc. TC4 IMEKO/IX Semetro*, Brazil, 2011.
- [17]. *IEEE Std 80 Guide for safety in AC substation grounding* – IEEE. New York, John Wiley, 2000.
- [18]. William H. Hayt Jr. and John A. Buck, "Engineering electromagnetics," McGraw-Hill, 8<sup>o</sup> Ed., New York. 2006.
- [19]. M. N. O. Sadiku, "A simple introduction to finite element analysis of electromagnetics problems", *IEEE Trans. Educ.*, vol. 32, no. 2, pp. 85- 9, 1989.
- [20]. BEAGLEBOARD.ORG. Beagleboard. [Online; accessed 17-11- 2011]. site:<http://beagleboard.org/>.